In Situ Synthesis of Iron Oxide Nanoparticles on Poly(ethylene oxide) Nanofibers Through an Electrospinning Process

Reza Faridi-Majidi, Naser Sharifi-Sanjani

School of Chemistry, University College of Science, Tehran University, Tehran, Iran

Received 13 November 2006; accepted 29 January 2007
DOI 10.1002/app.26230
Published online 23 April 2007 in Wiley InterScience (www.interscience.wiley.com).

ABSTRACT: Iron oxide nanoparticle coated poly(ethylene oxide) nanofibers as organic–inorganic hybrids with 200–400-nm diameters were prepared by the *in situ* synthesis of iron oxide nanoparticles on poly(ethylene oxide) nanofibers through the electrospinning of a poly(ethylene oxide) solution having Fe^{2+} and Fe^{3+} ions in a gaseous ammonia atmosphere. Transmission electron microscopy analysis proved the presence of iron oxide nanoparticles on the polymer nanofibers. The thermal properties of the nanofiber mat were also studied with differential scanning calorimetry and thermogravimetric analysis techniques. X-ray diffraction showed that the formed iron oxide nanoparticles were maghemite nanoparticles. The results were compared with those of the electrospinning of a poly(ethylene oxide) solution having Fe^{2+} and Fe^{3+} ions and a pure poly(ethylene oxide) solution in an air atmosphere. © 2007 Wiley Periodicals, Inc. J Appl Polym Sci 105: 1351–1355, 2007

Key words: fibers; nanoparticles; nanotechnology; poly (phenylene oxide); synthesis

INTRODUCTION

Electrospun nanofiber technology bridges the gap between deterministic laws (Newton mechanics) and probabilistic laws (quantum mechanics).[1] Because electrospun nanofibers with diameters within 100 nm are closer in scale to the quantum world than to the ordinary world, they frequently display quantum-like properties and have many fascinating nanoeffects.[1,2] Polymer, composite, and ceramic electrospun nanofibers with diameters as small as several tens of nanometers can be prepared by the electrospinning method, which is remarkably simple, versatile, and capable of producing nano- and microscale fibers in large quantities.[3] In electrospinning, a high electrostatic voltage is imposed on a drop of a polymer solution held by its surface tension at the end of a capillary tube. The surface of the liquid is distorted into a conical shape known as a Taylor cone.[4] Once the voltage exceeds a critical value, the electrostatic force overcomes the solution surface tension, and a stable liquid jet is ejected from the cone tip. Unlike conventional spinning, the jet is stable only near the tip of the spinneret, after which the jet is subject to instability (concluding axisymmetric and bending instabilities).[5,6] The solvent evaporates as the jet travels through the air, leaving behind ultrafine polymeric fibers collected on an electrically grounded target. The jet often follows a bending or spiral track resulting from the interaction between the external electric field and the surface charge of the jet. The jet instabilities not only result in the electrospinning jet being elongated up to ultrafine fibers but also lead to the formation of randomly deposited nonwoven electrospun fiber mats. Electrospun mats have a larger specific surface area and small pore size in comparison with commercial nonwoven fabrics. They are of interest in a wide variety of potential applications, including semipermeable and superhydrophobic membranes, nanocomposites, filters, protective clothing, coatings, conductive and semiconductive composites and nanowires, separators or electrolytes in rechargeable batteries, sensors, superparamagnetic and magnetic nanofibers, catalyses, nanocomposite films, wound dressings, tissue engineering scaffolds, and biosensing.[7–16]

It is also possible to produce functional polymer/metal oxide composite nanofibers having optical, electrical, or catalytic properties by the incorporation of metal oxide nanoparticles into them through the electrospinning process. Most of the reported manufacturing methods for polymer/metal oxide nanoparticle composite nanofibers are based on the electrospinning of a polymer solution blended with metal oxide nanoparticles. For example, Wang and coworkers produced superparamagnetic polymer nanofibers (which can be used in potential applications such as

Correspondence to: R. Faridi-Majidi (refaridi@khayam.ut.ac.ir).

TABLE I
Recipes for the Electrospinning Methods

Experiment	$FeCl_3 \cdot 6H_2O$ (g)	$FeSO_4 \cdot 7H_2O$ (g)	PEO (g)	Atmosphere	Atmosphere gas rate (L/min)
1	1.20	0.80	5.0	NH_3	10
2	1.20	0.80	5.0	Air	—
3	—	—	5.0	Air	—

magnetic filters,[17] sensors,[18] and future generations of electronic, magnetic, and/or photonic devices used for information storage, magnetic imaging, static and low-frequency magnetic shielding, and magnetic induction) by electrospinning poly(ethylene oxide) (PEO) and poly(vinyl alcohol) solutions containing dispersed magnetic iron oxide nanoparticles.[19] Another way of preparing polymer/metal oxide composite nanofibers is based on the electrospinning of a polymer precursor having metal ions and the subsequent posttreatment of the produced nanofibers. For example, electrospinning a polymer solution containing a TiO_2 precursor and subsequently immersing the produced electrospun composite nanofibers in deionized water led to the hydrolysis of the inorganic precursor on the surface of the nanofibers and produced polymer/titanium dioxide composite nanofibers.[20]

In this work, we are reporting a new method for producing polymer/metal oxide composite electrospun nanofibers. Thus, polymer/iron oxide nanoparticle nanofibers as organic–inorganic hybrids were prepared by the *in situ* synthesis of iron oxide nanoparticles on PEO nanofibers via the reaction of the traveling jet in electrospinning with an active atmosphere. Extensive characterization of the produced nanofibers was carried out with transmission electron microscopy (TEM), X-ray diffraction (XRD), differential scanning calorimetry (DSC), and thermogravimetric analysis (TGA) techniques, and the results were compared with those from electrospinning a PEO solution having Fe^{2+} and Fe^{3+} ions and a pure PEO solution in an air atmosphere.

EXPERIMENTAL

Materials

PEO with an average weight-average molecular weight of 900,000 was purchased from Acros Organics Co. (Noisy LeGrand, France). $FeCl_3 \cdot 6H_2O$, $FeSO_4 \cdot 7H_2O$, ammonium hydroxide (25%), and gaseous ammonia in a cylinder were purchased from Merck Chemical Co. (Whitehouse Station, NJ). Distilled water was used in all the experiments.

Electrospinning

Iron oxide nanoparticle coated PEO nanofibers were produced via an *in situ* electrospinning procedure with the following method: The given amounts (in Table I) of $FeCl_3 \cdot 6H_2O$ and $FeSO_4 \cdot 7H_2O$ were dissolved in 100 mL of distilled water, and then 5.0 g of PEO was added to this solution, which was left for 2 nights to obtain a homogeneous polymer solution. The polymer solution was put into a hypodermic syringe. A syringe pump (supplied by Stoelting Co., Wood Dale, IL) was used to feed the polymer solution into a metallic needle with an inner diameter of 0.7 mm. A grounded aluminum foil as a collector was located at a fixed distance of 21 cm from the needle. The metallic needle and the collector were enclosed in a poly(methyl methacrylate) box ($40 \times 50 \times 60$ cm^3). The feed rate of the syringe pump was fixed at 1.1 mL/h. A positive potential of 17.5 kV was then applied to the polymer solution with a high-voltage power supplier (MH 100 series, supplied by HiTek Power Co., Littlehampton, West Sussex, UK). During electrospinning, gaseous ammonia (from a cylinder purchased from Merck Chemical) was purged into the box at a rate of 10 L/min. Electrospun nanofibers were collected on the surface of the aluminum foil. The recipe and the amounts of the materials used in this experiment are shown in Table I (no. 1).

For comparison, the electrospinning of the aforementioned PEO solution having iron ions (no. 2) and a pure PEO solution in an air atmosphere (no. 3) was also carried out in a way similar to that for no. 1, excluding the box. The recipes and the amounts of the materials used in these experiments are also given in Table I. All electrospinning was performed under room conditions at about 27–32°C and 20–30% humidity.

Characterization

A Zeiss CEM 902A (Oberkochen, Germany) transmission electron microscope with an accelerating voltage of 80 kV was used to obtain information about the morphology and size of the nanofibers. The electrospun nanofibers were directly deposited onto a copper grid and then analyzed by the TEM technique.

The thermal properties of the electrospun fibers were analyzed by TGA (model TGAQ50, TA Instruments, New Castle, DE) at a heating rate of 20°C/min and by DSC (model DSCQ100, TA Instruments) at a heating rate of 10°C/min under inert Ar gas.

XRD patterns of the samples were recorded by a Seifert XRD 3003 PTS diffractometer (GE Inspection

Technologies, Hurth, Germany); scans were made from 5 to 90° (2θ). The nanofiber mats were deposited onto glass during electrospinning and then analyzed by an XRD method.

RESULTS AND DISCUSSION

Three electrospinning reactions (nos. 1–3) were carried out; a brown nanofiber mat was obtained in no. 1, a light brown nanofiber mat was obtained in no. 2, and a white nanofiber mat was obtained in no. 3. A comparison of the appearance of the mat obtained from no. 1 with that of the other mats obtained from nos. 2 and 3 suggested that the iron ions in the jet traveling the distance between the needle and collector could precipitate in the gaseous ammonia atmosphere to produce iron oxide. To prove this hypothesis and study the morphology and size of the produced nanofibers, the electrospun nanofibers were analyzed by the TEM technique. Figure 1 presents the TEM image of nanofibers obtained from no. 1, and as it shows, dark spots were dispersed heterogeneously on the nanofibers as a shell. The TEM image of the nanofibers obtained from the electrospinning of the PEO solution containing iron ions in an air atmosphere (no. 2; Fig. 2) showed that there were homogeneous, dark spots in the nanofibers in the experiment. A comparison of these two images (Figs. 1 and 2) indicates that in experiment no. 1, iron oxide nanoparticles were heterogeneously synthesized on the nanofibers by the precipitation of iron ions in the ammonia atmosphere (as it is well known, iron oxide nanoparticles can be synthesized by the coprecipitation of aqueous iron ions with a base such as ammonia),[21,22]

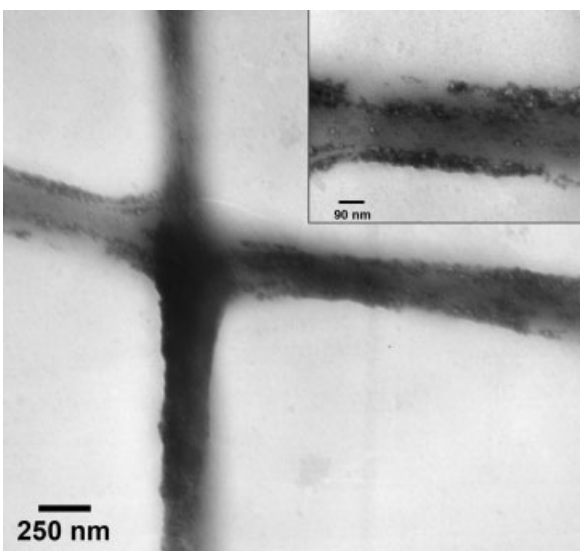

Figure 1 TEM micrograph of nanofibers obtained in the electrospinning of a PEO solution having iron ions in an NH_3 atmosphere (no. 1).

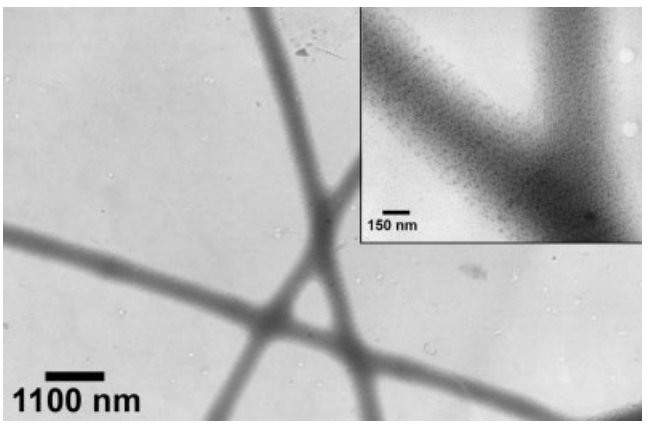

Figure 2 TEM micrograph of nanofibers obtained in the electrospinning of a PEO solution having iron ions in an air atmosphere (no. 2).

whereas in experiment no. 2, iron salt nanoparticles were formed in the nanofibers during electrospinning via solvent evaporation in this process. TEM analysis, as shown in Figure 3, did not show either of these two events for no. 3 (nanofibers obtained from the electrospinning of a pure PEO solution in an air atmosphere). These TEM micrographs (Figs. 1–3) also show that the produced nanofibers in the three experiments had diameter ranges of about 200–400 nm.

The thermal properties of the nanofiber mats produced in the experiments (nos. 1–3) were analyzed by DSC analysis to study the first-order transition of melting and the crystallization of the nanofibers. Figure 4 summarizes DSC thermograms of the produced nanofiber mats in nos. 1–3. Curves A, B, and C in Figure 4 are the DSC thermograms of the nanofiber mats obtained from the electrospinning of a pure PEO solution (no. 3), a PEO solution having iron ions in an ammonia atmosphere (no. 1), and a PEO solution having

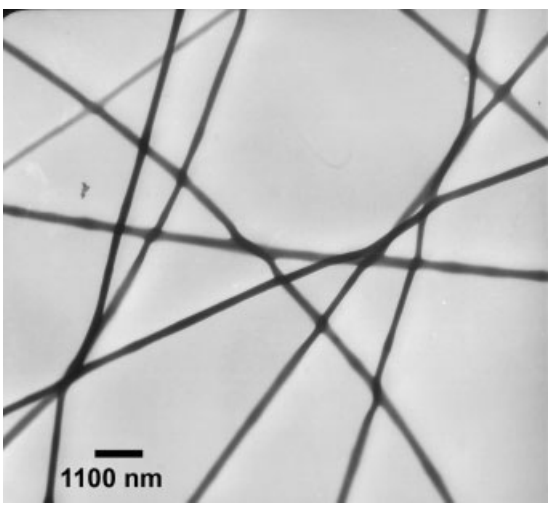

Figure 3 TEM micrograph of nanofibers obtained in the electrospinning of a pure PEO solution (no. 3).

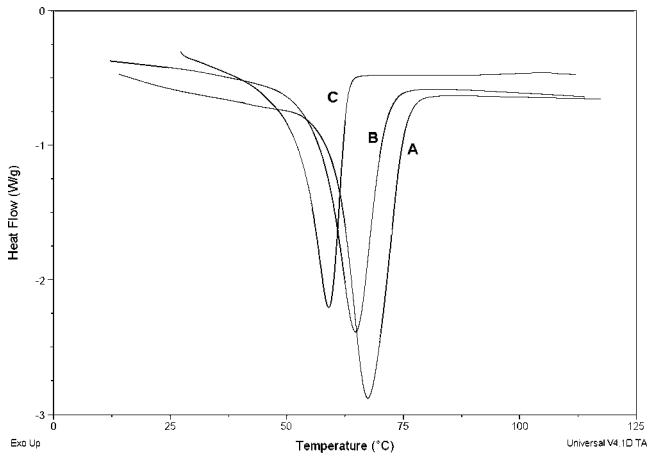

Figure 4 DSC thermographs of the nanofiber mats produced in the experiments: (A) no. 3, (B) no. 1, and (C) no. 2.

iron ions in an air atmosphere (no. 2), respectively. The presence of an intense melting peak in the DSC thermograms indicates the semicrystalline products. This figure shows that the melting point of the nanofibers in curve C (no. 2) is lower than that in curve B (no. 1), and the melting point of the nanofibers in curve B is lower than that in curve A (no. 3). This is a result of the higher proportion of iron salts in the nanofibers produced in no. 2 than in the nanofibers produced in no. 1 due to the reaction of some of the iron ions with the ammonia medium, which formed iron oxide nanoparticles in no. 1 rather than iron salt nanoparticles by the evaporation of the solvent (water) during jet travel in the process. The proportion of the iron salts in the nanofibers produced in experiment no. 1 was also higher than that of the pure PEO nanofibers produced in experiment no. 3. The melting points of the products are listed in Table II. From the DSC analyses, the crystallinity (X_c) percentages of the nanofiber mats (obtained in nos. 1–3) were calculated with the following equation: X_c (%) $= (\Delta H_f/\Delta H_f^0) \times 100$, where ΔH_f^0 is the heat of fusion of completely crystalline PEO (213.7 J/g)[23] and ΔH_f is the heat of fusion for the sample. The ΔH_f and X_c values of the nanofiber mats are also presented in Table II. As shown in Table II, all the nanofibers are semicrystalline, and the crystallinity of the nanofibers, like the melting point, decreases with the increase in the iron salt proportion. For comparison, the virgin PEO powder used in this work was also analyzed by DSC analysis, and the meting point, ΔH_f, and X_c values are also presented in Table II. A comparison of the melting point and X_c of the PEO powder with those of pure PEO nanofibers (obtained in no. 3) shows that the melting point is constant but X_c is significantly reduced in the nanofiber production process (see Table II).

TABLE II
Melting Points, ΔH_f Values, and X_c Values of the Produced Nanofibers and Virgin PEO Powder

Experiment	Melting point (°C)	ΔH_f (J/g)	X_c (%)
1	54.2	110.6	51.75
2	49.1	86.8	40.62
3	60.1	130.8	61.21
Powder PEO	60.5	166.0	77.68

The thermal properties of the nanofiber mats produced in the experiments (nos. 1–3) were also analyzed by TGA. Figure 5 presents the TGA thermograms of the nanofiber mats. Curves A, B, and C in Figure 5 are TGA plots of nanofiber mats obtained in experiments nos. 3, 1, and 2, respectively. As curve A in this figure (TGA thermogram of the no. 3 nanofibers) shows, the pure PEO nanofiber mat is decomposed at 352°C, whereas curves B and C (the TGA thermograms of nos. 1 and 2, respectively) show the first weight loss after 100°C due to the loss of the hydrated water of the hydrated iron salts in the nanofibers and the second weight loss at about 250°C due to the decomposition of the polymer chain in the presence of the salt nanoparticles and the iron oxide nanoparticles, which accelerate the decomposition of PEO. TGA of the nanofibers produced in nos. 1 and 2 (Fig. 5) also shows a residue (at ca. 16%), which is remarkable in comparison with the pure PEO nanofiber, which shows a small residue (at ca. 2.5%) at 500°C. The virgin PEO powder was also analyzed by TGA, and it showed that its results were similar to those of pure PEO nanofibers (obtained in no. 3).

The XRD patterns of the nanofibers obtained from the experiments (nos. 1–3) are given in Figure 6. An initial conclusion could be that the patterns in this figure are different. The two strong peaks appearing at 2θ values of about 19 and 23° in Figure 6(a) (pure PEO nanofibers obtained from no. 3) are assigned to crystalline PEO.[24] The intensities of these peaks were significantly reduced in the product of the electro-

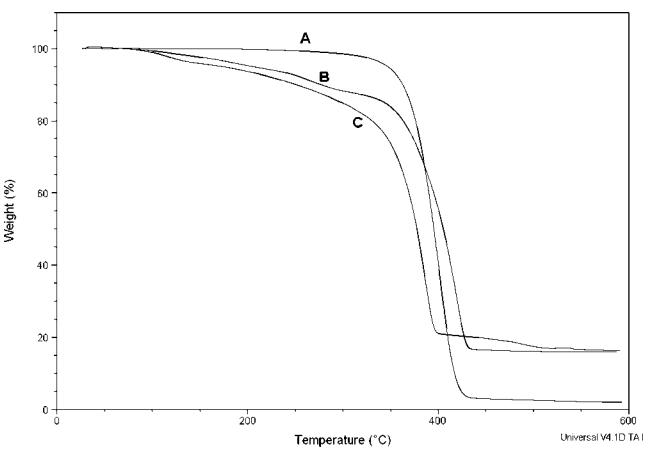

Figure 5 TGA thermographs of the nanofiber mats produced in the experiments: (A) no. 3, (B) no. 1, and (C) no. 2.

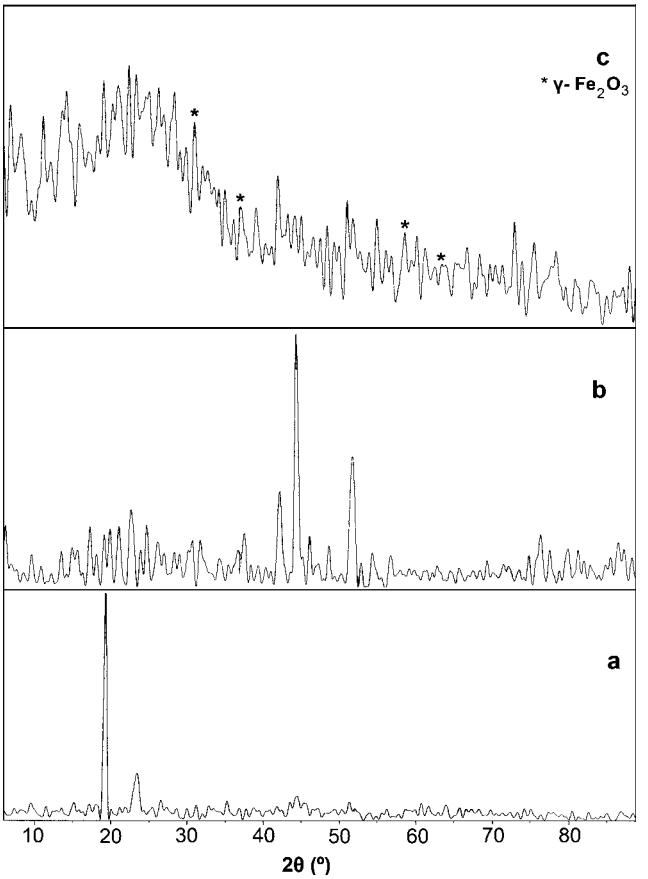

Figure 6 XRD patterns of the nanofiber mats produced in the experiments: (a) no. 3, (b) no. 2, and (c) no. 1.

spinning of the PEO solution having iron salts in an air atmosphere (no. 2), as shown in Figure 6(b). This point indicates the reduction of the PEO crystallinity, which was quantitatively studied by DSC analysis, as previously mentioned. The XRD pattern of the product obtained in no. 1 [Fig. 6(c)] displays some peaks at 2θ values of 31.1, 36.5, 58.7, and 63.8°, which are related to maghemite (γ-Fe_2O_3) lattice forms corresponding to scattering forms of (2 2 0), (3 1 1), (5 1 1), and (4 4 0), respectively,[25] which are not present in Figure 6(b) (the product obtained in the electrospinning of a PEO solution having iron ions in an air atmosphere, i.e., no. 2).

CONCLUSIONS

Iron oxide nanoparticle coated PEO nanofibers were prepared by the *in situ* synthesis of iron oxide nanoparticles as organic–inorganic hybrids on PEO nanofibers through the electrospinning of a solution of PEO having Fe^{2+} and Fe^{3+} ions in a gaseous ammonia atmosphere. TEM showed the polymer nanofibers to be 200–400 nm in diameter, and it also proved the presence of the nanoparticles on the polymer electrospun nanofibers. DSC analysis showed that X_c of the PEO nanofibers diminished in the presence of iron salt nanoparticles. XRD analysis showed that the nanoparticles that formed on the nanofibers were γ-Fe_2O_3 nanoparticles. This work shows that a traveling polymer jet in electrospinning can react with an active atmosphere, and this procedure has potential implications for the easy production of organic–inorganic hybrid nanofibers and nanostructures that can be used in several useful applications.

The authors express their special gratitude to Madani for his painstaking aid in the laboratory, Hashemi for obtaining transmission electron micrographs in the Laboratory of Electronic Microscopy at the University College of Science of the University of Tehran, and Norouzi.

References

1. He, J. H.; Wan, Y.-Q.; Xu, L. Chaos Soliton Fract 2007, 33, 26.
2. He, J. H.; Liu, Y.; Xu, L.; Yu, J. Y. Chaos Soliton Fract 2007, 32, 1096.
3. Hong, K. H.; Kang, T. J. J Appl Polym Sci 2006, 100, 167.
4. Taylor, G. I. Proc R Soc London 1969, 313, 453.
5. He, J. H.; Wan, Y. Q.; Yu, M. Y. Int J Nonlinear Sci Numer Simul 2004, 5, 243.
6. He, J. H.; Wu, Y.; Zuo, W. W. Polymer 2005, 46, 12637.
7. Ramakrishna, S.; Fujihara, K.; Teo, W.-E.; Yong, T.; Ma, Z.; Ramaseshan, R. Mater Today 2006, 9, 40.
8. Ma, M. L.; Hill, R. M.; Lowery, J. L.; Fridrikh, S. V.; Rutledge, G. C. Langmuir 2005, 21, 5549.
9. Qin, X.-H.; Wang, S.-Y. J Appl Polym Sci 2006, 102, 1285.
10. Wang, X.; Fang, D.; Yoon, K.; Hsiao, B. S.; Chu, B. J Membr Sci 2006, 278, 261.
11. Hong, K. H.; Kang, T. J. J Appl Polym Sci 2006, 99, 1277.
12. Babel, A.; Li, D.; Xia, Y.; Jenekhe, S. A. Macromolecules 2005, 38, 4705.
13. Zhu, Y.; Zhang, J. C.; Zhai, J.; Jiang, L. Thin Solid Films 2006, 510, 271.
14. Wang, M.; Singh, H.; Hatton, T. A.; Rutledge, G. C. Polymer 2004, 45, 5505.
15. Demir, M. M.; Gulgun, M. A.; Menceloglu, Y. Z.; Erman, B.; Abramchuk, S. S.; Makhaeva, E. E.; Khokhlov, A. R.; Matveeva, V. G.; Sulman, M. G. Macromolecules 2004, 37, 1787.
16. Wang, Y.; Yang, Q.; Shan, G.; Wang, C.; Du, J.; Wang, S.; Li, Y.; Chen, X.; Jing, X.; Wei, Y. Mater Lett 2005, 59, 3046.
17. Pinchuk, L. S.; Markova, L. V.; Gromyko, Y. V.; Markov, E. M.; Choi, J. Mater Process Technol 1995, 55, 345.
18. Epstein, A. J.; Miller, J. S. Synth Met 1996, 80, 231.
19. Wang, M.; Singh, H.; Hatton, T. A.; Rutledge, G. C. Polymer 2004, 45, 5505.
20. Hong, Y. L.; Li, D. M.; Zheng, J.; Zou, G. T. Nanotechnology 2006, 28, 1986.
21. Zheng, W.; Gao, F.; Gu, H. J Magn Magn Mater 2005, 288, 403.
22. Faridi-Majidi, R.; Sharifi-Sanjani, N.; Agend, F. Thin Solid Films 2006, 515, 368.
23. Xi, J.; Tang, X. Chem Phys Lett 2004, 393, 271.
24. Xi, J.; Qiu, X.; Zhu, W.; Tang, X. Microporous Mesoporous Mater 2006, 88, 1.
25. Sun, Y.-K.; Ma, M.; Zhang, Y.; Gu, N. Colloids Surf A 2004, 245, 15.